The construction of movement by the spinal cord

Matthew C. Tresch[1,2], Philippe Saltiel[1] and Emilio Bizzi[1]

[1] *Department of Brain and Cognitive Sciences, Massachusetts Institute of Technology, E25–526, Cambridge, Massachusetts 02139, USA*

[2] *Present address: Section of Neurophysiology, Panum Institute, University of Copenhagen, Copenhagen, Denmark*

Correspondence should be addressed to E.B. (emilio@ai.mit.edu)

We used a computational analysis to identify the basic elements with which the vertebrate spinal cord constructs one complex behavior. This analysis extracted a small set of muscle synergies from the range of muscle activations generated by cutaneous stimulation of the frog hindlimb. The flexible combination of these synergies was able to account for the large number of different motor patterns produced by different animals. These results therefore demonstrate one strategy used by the vertebrate nervous system to produce movement in a computationally simple manner.

The ease with which we move in and interact with our environment belies the complexity inherent in even the simplest of these tasks. Movements we make effortlessly, such as reaching for an object or walking over uneven terrain, involve the specification and control of a vast number of variables[1], ultimately involving the activation of many thousands of motor units spanning dozens of muscles. The question of how the nervous system overcomes these complexities to produce movement effortlessly and efficiently is central to the study of the neural control of movement.

We describe one strategy used by the vertebrate nervous system to produce a range of behavior in a simple manner. We show that the neural circuitry within the frog spinal cord produces motor responses to hindlimb cutaneous stimulation by the combined recruitment of a small number of distinct muscle groups. Such a muscle group, in which the activation level of a set of muscles is specified together, has been termed a 'muscle synergy' previously[2,3]. Several researchers have proposed that such spinally organized muscle groupings might underlie the production of movement[4–7]. The present results provide direct support for these proposals, presenting a quantitative assessment of a testable form of this hypothesis. These experiments thus provide a novel perspective on this fundamental question of how the vertebrate nervous system produces movement in a simple and efficient manner.

Results

We examined the patterns of muscle activations evoked from cutaneous stimulation of the hindlimb of spinalized frogs (frogs whose spinal cord was transected). We stimulated a number of different skin locations to evoke a range of motor responses, to try to understand how this range was produced by the nervous system. An example of the muscle activation patterns (**Fig. 1b**) evoked from stimulating different regions (**Fig. 1a**) along the rostral and caudal margins of the hindlimb is shown for one animal. The activation level of the majority of muscles in each frog was significantly dependent on the stimulus location on the leg ($p < 0.05$, ANOVA). This dependency caused the production of a range of different muscle activation patterns. Stimulation of sites on the back of the calf (regions 1–4) typically evoked responses with a strong activation of vastus externus (VE) with a weaker activation of a few other muscles, such as biceps femoris (BF), iliopsoas (IP) or adductor magnus (AM). Stimulation of sites on the foot (regions 5–10) typically evoked responses with a strong activation of semitendinosus (ST) and IP and weaker activation of other muscles such as sartorius (SA), rectus internus (RI), AM, vastus internus (VI) and BF. As the stimulation site was moved along the front of the calf toward the knee (regions 11–14), the contribution of ST gradually decreased, whereas the contribution of other muscles, particularly SA and AM gradually increased ($n = 7$).

We examined whether these responses were produced from the combination of distinct groups of muscles. Such muscle groups might be observed either in the variations among responses evoked from different skin regions (as shown in **Fig. 1b**), or in the variations among responses evoked from the same skin location (as shown in **Fig. 2a**; each of these five responses were evoked from stimulation of the front of the calf near the knee indicated in **Fig. 1a**). Although the averaged and normalized responses (**Fig. 2b**) were generally similar to one another, there were clear systematic differences between them. For instance, the fourth and fifth responses were very similar except that there was a stronger activation of BF and IP in the fifth response. In the first and second responses, the activation of ST was very similar, but there was a weaker activation of SA, AM, VI, BF and IP in the second response. These comparisons suggest the existence of a set of at least three groups of muscles that could be controlled independently: one with activation of ST, one with activation of SA, AM and VI, and one with activation of BF and IP.

We investigated more systematically whether the patterns of muscle covariations shown in Fig. 2b and the range of muscle activations shown in Fig. 1a could both result from the combination of a small number of muscle activation patterns or muscle synergies. An explicit formulation of this hypothesis has been proposed[8,9,10], and we evaluated this formulation here. According to this hypothesis, any given response should be describable as the linear combination of a small number of such muscle synergies. Further, both the elements of the synergies and their weighting within each response should be positive, because we

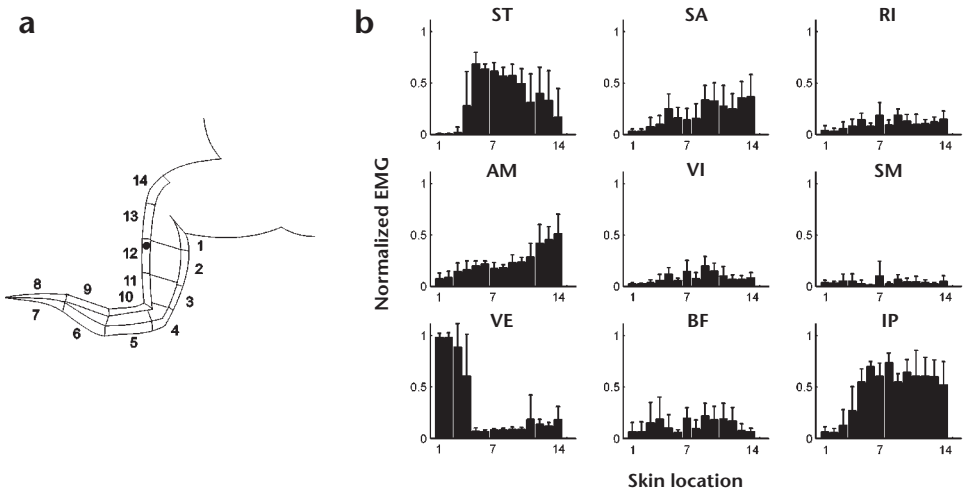

Fig. 1. Muscle activation patterns evoked from cutaneous stimulation of the frog hindlimb. **(a)** The divisions of stimulation sites used to examine the variation of muscle activation patterns with stimulus location shown in (b). Stimulation was applied to many sites across the skin surface, and the evoked pattern of muscle activation was measured for each site. The hindlimb configuration shown here corresponds to the configuration used in these experiments. The dot within region 12 indicates the stimulus site from which the responses shown in Fig. 2a were evoked. **(b)** The variation of muscle activation with stimulus location for one animal. Stimulation sites on the back and front of the femur did not consistently evoke responses in each frog and so were excluded from analysis. The averaged, normalized activation for each recorded muscle is shown as a function of stimulus location. For this plot, we also normalized each observed response to be of unit magnitude (taken as the vector norm). The values here therefore reflect the relative contribution of each muscle to a given response. The numbers on the horizontal axis refer to the stimulus regions indicated in (a). Error bars represent one standard deviation from the mean activation level at each region. The data shown here were obtained from a total of 688 responses.

are ultimately considering muscle activations (Galagan, J. *et al. Soc. Neurosci. Abstr.* **23**, 512.4, 1997). This specific hypothesis can be formalized in the following model:

$$m_j^{obs} = \sum_{i=1}^{N} c_{ij} w_i \qquad c_{ij}, w_i \geq 0 \qquad (1)$$

where m_j^{obs} is the jth observed pattern of muscle activations, c_{ij} is the positive weighting coefficient of the ith muscle synergy for the jth response, w_i is the ith muscle synergy and N is the number of muscle synergies. We tested how well this positive linear combination of muscle synergies model explained the patterns of muscle activations observed experimentally.

We extracted a set of muscle synergies from the observed muscle activations for each animal using a computational analysis. This analysis aimed at finding the set of muscle synergies that could best predict the observed responses according to the model described above. Briefly, the algorithm began with a set of arbitrary synergies, w_i. The positive weighting coefficients of these arbitrary synergies, c_{ij}, that best predicted each response were then found. The muscle synergies were updated by performing a gradient descent on the error between the observed response and the best-fit, predicted response. This process was then iterated until the algorithm converged on a particular set of muscle synergies.

In a typical animal (**Fig. 2c**), the algorithm extracted both a set of synergies and the weighting coefficients of each synergy used to reconstruct the responses evoked from cutaneous stimulation. The algorithm extracted a synergy with ST, a synergy with SA, AM and VI, a synergy with VE, and a synergy with BF and IP. These synergies corresponded well to the patterns of covariation observed in Fig. 2b. The derived synergies were very robust to differences in initial conditions, with an average normalized dot product of .97 ± .04 between the synergies found on different iterations of the algorithm. Qualitatively, the observed (**Fig. 2b**) and predicted (**Fig. 2d**) responses were very similar to one another. Quantitatively, this similarity between observed and predicted responses was found to be very large for each animal. In each of the seven animals examined here, with an average of 392 responses per animal, the algorithm consistently explained a large amount of variance in the patterns of muscle activations (mean $r^2 = .90 \pm .03$).

The synergies shown in Fig. 2c were generally similar between animals. The average similarity (calculated as the normalized dot product) between synergies found in different animals was .74 ± .20. The similarity of the first three synergies shown in Fig. 2c was generally higher than that of the fourth (.91 ± .09, .80 ± .11, .80 ± .22, .45 ± .28, respectively). This similarity, however, was less than the similarity between synergies found on repeated iterations of the algorithm for the same animal (.74 versus .97), suggesting that there were differences between the synergies found in different animals. Differences in such factors as electrode placements, link lengths or possibly the strategies used by different animals could have contributed to these differences.

We compared the results obtained by this algorithm to the results obtained by the k-means algorithm[11,12]. K-means attempts to explain each observed response as one of only a small number of possible responses. In contrast to our algorithm, k-means does not allow an observed response to be a combination of more basic patterns; in k-means, each response reflects the recruitment of a single pattern. To explain 90% of the variance in the observed set of responses, k-means required at least 15 different patterns. This demonstrates that cutaneous stimulation of the hindlimb did not simply evoke only a few distinct types of muscle patterns. Instead, the range of responses evoked from cutaneous stimulation was better explained as the combination of a small number of muscle synergies.

We also examined how the results of the algorithm explained the range of muscle activation patterns evoked from different regions of the skin, such as those shown for the animal in Fig. 1b. We show for three animals how the weighting coefficient of each synergy extracted by the algorithm varied with the stimulus location on the hindlimb (**Fig. 3**). These are the weighting coefficients of the synergies used to reconstruct each response (**Fig. 2c**). For instance, in the animal shown in Fig. 3a, to recon-

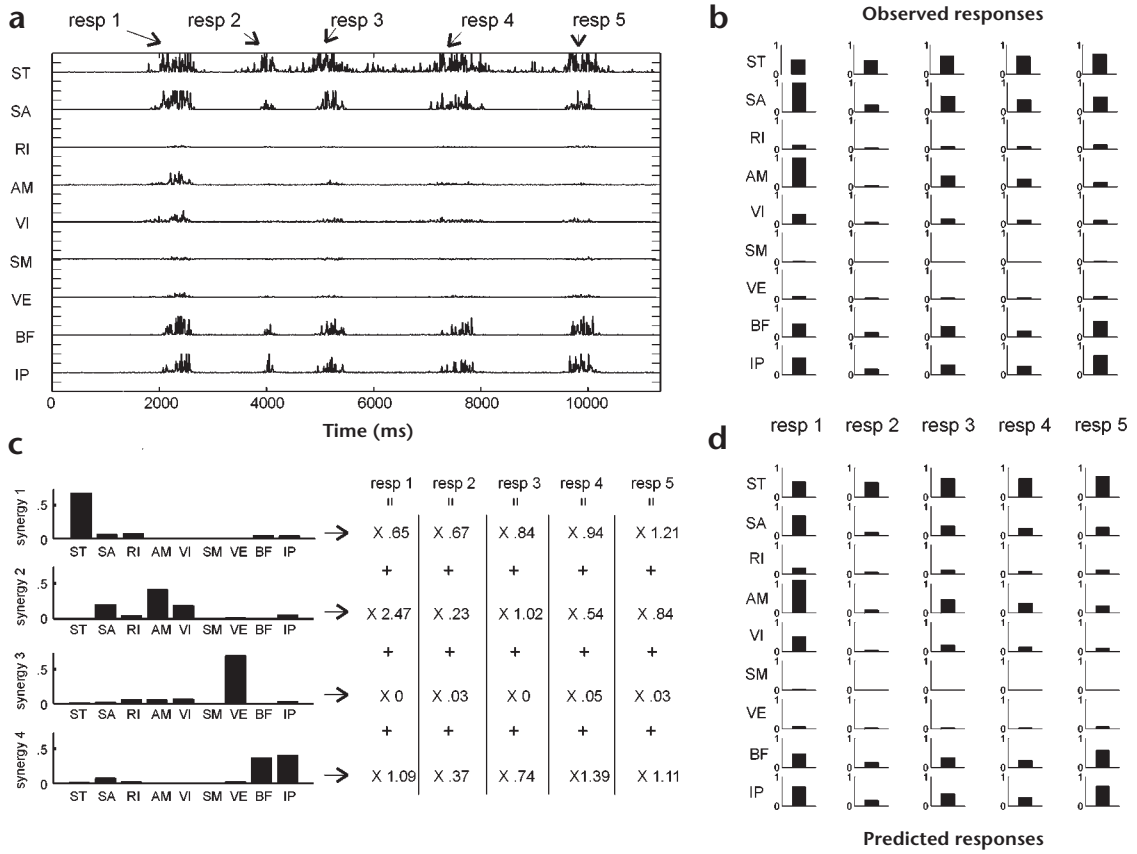

Fig. 2. Example of muscle covariation patterns within evoked responses. **(a)** Raw EMGs for five responses evoked from stimulation of the same skin region. The hindlimb was fixed in the configuration shown in Fig. 1a for all responses and the region of the skin indicated in Fig. 1a was stimulated using a handheld probe (see Methods). **(b)** Averaged, normalized activation for the muscles recorded in each of the responses shown in (a). Note that each muscle was normalized to the maximal value observed for that muscle across all responses evoked from any stimulation site in this animal. As a result, the muscle balances seen in (a) are slightly different than those shown in (b). **(c)** Responses can be explained as a linear combination of a set of muscle synergies. The synergies obtained from applying the algorithm described in the text to the entire set of responses obtained from this animal are shown to the left. The weightings of each of these synergies used to reconstruct the responses in (b) are shown to the right. For instance, the first response was reconstructed as .65 of the first synergy, plus 2.47 of the second synergy, 0 of the third synergy, and 1.09 of the fourth synergy. **(d)** Responses resulting from the combination of muscle synergies shown in (c).

struct responses from sites of the back of the leg (regions 1–4), the algorithm used a strong weighting of the synergy with VE (the third synergy in **Figs. 2c** and **3a**). This strong VE activation is consistent with the responses observed from the back of the leg (**Fig. 1b**). Similarly, to reconstruct responses from sites on the foot (regions 5–10), the algorithm used a strong weighting of the synergy with ST (the first synergy in **Figs. 2c** and **3a**) along with weaker weightings of the synergy with SA, AM and VI (the second synergy in **Figs. 2c** and **3a**). As stimulation sites moved along the front of the leg (regions 11–14), the weighting of the synergy with ST gradually decreased, whereas the activation of the SA, AM and VI synergy and of the VE synergy increased. Activation of the fourth synergy was more variable across regions of the skin surface. Generally similar patterns of recruitment of synergies were observed in each animal (compare **Fig. 3a, b** and **c**).

Although Fig. 3 suggests that the use of each type of synergy was generally similar in each animal, the exact pattern of recruitment of these synergies could differ between animals. In the animal shown in Fig. 3c, for instance, there were sharp transitions in the weighting of each synergy between different skin regions. These sharp transitions were especially clear for the first three synergies, with the weighting coefficients of these synergies either being zero or large for most responses. In the animals shown in Fig. 3a and 3b, however, there appeared to be more of a gradual transition in the recruitment of different synergies, as indicated in the more intermediate weighting coefficients of each synergy. This type of gradual transition was seen in most animals, especially for the transition from the foot to the front of the leg. These observations suggest that each animal has access to a similar set of muscle synergies when producing responses to cutaneous stimulation, but that there is a degree of flexibility in the exact pattern of their use.

Finally, we examined the generality of the synergies derived from the responses evoked from stimulation of the sites shown in Fig. 1a. We examined how well these synergies were able to explain the responses evoked from other regions of the skin surface; if similar synergies were used to produce responses from these other regions, we would expect the responses to be explained well by these synergies. We evoked responses from stimulation of sites on the dorsal surface of the foot, the dorsal surface of the calf, the contralateral ankle, the ipsilateral and contralateral back and both forelimbs. The synergies obtained from

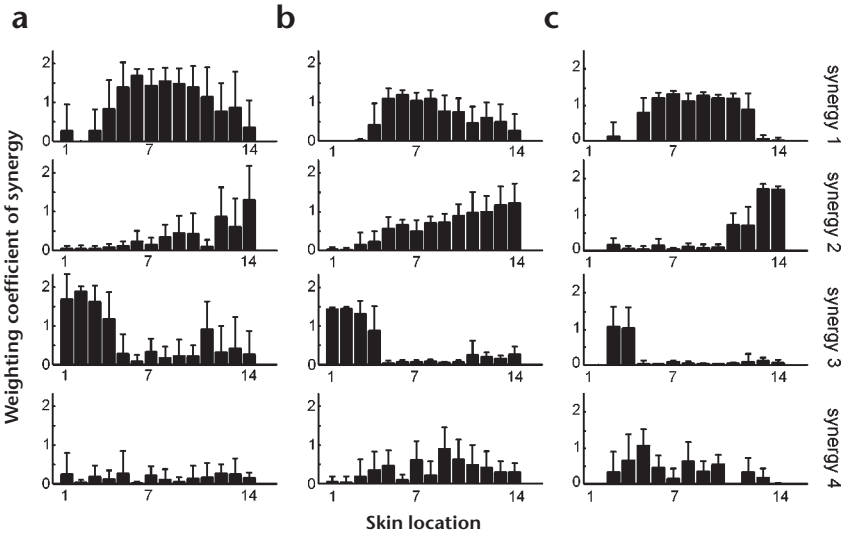

Fig. 3. The contribution of each muscle synergy to responses evoked from different regions of the skin surface for three different animals **(a, b, c)**. The order of the synergies shown here corresponds to the order of the synergies shown in Fig. 2c. The correspondence between synergies was made using the normalized dot product between them. The numbers on the horizontal axis refer to the regions shown in Fig. 1a. The vertical axis shows the average weighting coefficient for each muscle synergy used to reconstruct the observed responses, such as those shown in Fig. 1b.

stimulation of the hindlimb were able to explain over 80% of the variance in the responses evoked from sites on the dorsal surface of the foot and calf, the ipsilateral back and the contralateral ankle (**Fig. 4**). Responses from the other skin regions, however, were not well explained by these same synergies. The observation that the synergies explained some responses poorly also demonstrates that the synergies were not so general as to be able to explain any possible motor response. These results suggest that the synergies used to produce the responses from the hindlimb might also be used in the motor responses evoked through other pathways.

Discussion

These results demonstrate that the neural circuitry within the vertebrate spinal cord seems to produce a behavior through the combination of a small number of muscle synergies. By using a computational analysis, we show that such a combination of muscle synergies is able to explain the range of muscle activations evoked by cutaneous stimulation of the frog hindlimb. Such a strategy of combining a small number of basic motor elements greatly simplifies the complexity intrinsic to the production of movement by the nervous system.

These results provide direct support for previous hypotheses of the production of movement by the spinal cord[4–6]. For instance, the nervous system was proposed to produce a range of movement through the combination of a small number of 'unit burst generators' organized within the spinal cord[5]. Each of these unit bursters was proposed to control the activation of a small group of synergistic muscles. These units could then be coupled in many different ways to produce a wide range of behavior. The hypothesis considered here, that the spinal cord produces movement through the combination of a small number of motor elements, is similar to this unit burst generator hypothesis.

The main contribution of this study has been to state this hypothesis in an explicit form, allowing it to be examined quantitatively. The computational analysis described here provided a method to identify the basic elements underlying the production of movement in a systematic and objective manner. The consistency of the results of this algorithm with qualitative examination of the data helps to validate the approach used here. This explicit formulation of the hypothesis also allowed it to be falsified: the results of this algorithm could easily have failed to consistently explain the responses with the fidelity observed here. Further, the particular model we tested, as expressed in Eq. 1, was relatively simple, assuming a linear and independent combination of muscle synergies. This simplicity makes it all the more surprising that the model was able to explain these responses so well.

The results and methods of our study might be used to examine how the spinal cord is used by the rest of the nervous system to produce movement. We found that the set of synergies described here could explain some, but not all, of the responses evoked from other regions of the skin surface. This result suggested that these synergies might be utilized by different pathways in the production of movement. We might be able to use similar procedures to examine whether descending systems also use these synergies to produce movement. For instance, vestibular stimulation in the frog evokes a low-dimensional set of hindlimb movements[13]. It will be interesting to examine the relationship between the low dimensionality of that set of movements and the combination of a small number of muscle synergies identified here. Further, it will be important to examine whether the model described here is capable of explaining the complete time course of motor responses. In many behaviors, there is a great deal of temporal precision in muscle activation patterns[3], and it will be interesting to examine whether this precision can be described in terms of a small number of synergies. Further experiments

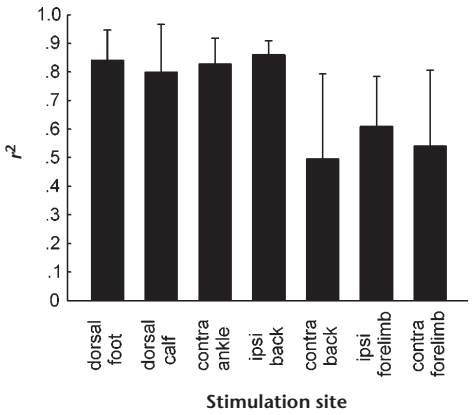

Fig. 4. The ability of synergies from sites on the rostral and caudal margins of the hindlimb to explain responses evoked from other skin regions. Synergies were derived from the regions shown in Fig. 1a and then used to describe the responses evoked from the other skin regions indicated on the horizontal axis. The vertical axis shows the r^2 values for the fits for each of these data sets.

will be required to define the extent and limits of the generality of the synergies described here to other behaviors, including those produced by descending systems.

Sherrington first proposed that the responses to cutaneous stimulation might also be used in other classes of movement, such as locomotion[4]. Although the movements produced by the spinal cord in response to cutaneous stimulation are often considered to be simple and stereotyped, it is well established that these responses can be precisely tuned depending on the site of stimulation[14–17]. This flexibility might be used in the movements produced by descending systems[18]. Our study might provide a novel perspective from which to test this hypothesis.

Methods

Data acquisition. All procedures were approved by the Committee on Animal Care at M.I.T. Seven adult frogs (*Rana catesbiana*) were spinalized at the level of the obex under tricaine anesthesia. Nine hindlimb muscles were implanted with bipolar EMG electrodes (see ref. 9 for details): semitendinosus (ST), sartorius (SA), rectus internus (RI), adductor magnus (AM), vastus internus (VI), semimembranosus (SM), vastus externus (VE), biceps femoris (BF) and iliopsoas (IP). In one animal, we recorded from rectus anterior in the place of IP. Crosstalk from electrical pickup between adjacent muscles was eliminated by suturing small pieces of insulation to the fascia in the majority of animals. The effectiveness of this insulation was confirmed by observing no EMG signals in muscles with their nerve supply cut. The hindlimb was fixed in the horizontal plane at the level of the hip by means of bone screws attached at the ankle and the metatarsus. This restraint prevented all movement of the hindlimb. The foot was fixed at a right angle relative to the calf (see **Fig. 1a**). The hindlimb was mechanically stimulated by scratching restricted sites on the skin surface (1 mm^2 tip, .01 to .1 N force, 1–4 Hz, over a range of 1–3 mm). Stimulation strength was regulated so as to evoke only threshold responses. EMG signals were filtered and amplified (25 k) before being digitally sampled (1 kHz) for offline analysis. Response onsets and offsets were identified offline using interactive software written in Matlab, and the activation level of each muscle was averaged within each response. The activation of each muscle was then normalized to the maximal value observed for that muscle in any response. Weak responses with a magnitude (taken as the vector norm) less than .3 were excluded from further analysis because EMG noise often obscured the balance of muscle activations in these weaker responses.

We assessed the repeatability of the stimulation procedures used here by examining the variability in the responses evoked from repeated stimulation of a site on the skin. The standard deviation in the most activated muscle in a response was .27 across all animals. This variability was comparable to the variability in the responses evoked from repeated electrical stimulation of the same site in spinal cord (standard deviation, 0.21, data not shown). Such electrical stimulation would be expected to activate the same neural substrate on each application of stimulation and should therefore give a lower bound of the variability in the motor responses evoked in this preparation. Such variability in the responses evoked in this preparation has been observed previously[19].

Algorithm to extract muscle synergies. A set of synergies, w_i, consists of coefficients chosen randomly between 0 and 1 for each muscle. We then approximated each observed response as a positive linear combination of these synergies, described by Eq. 1. A slightly different form of Eq. 1 in the actual fitting procedure was used to impose the restriction of the synergies to positive numbers.

$$m_j^{obs} \approx m_j^{pre} = \sum_{i=1}^{N} c_{ij} g(w_i) \qquad (1)$$

m_j^{obs} is the jth observed pattern of muscle activations, m_j^{pre} is the jth predicted pattern of muscle activations and $g(x)$ is a positive valued function of x. We tried several different forms of $g(x)$, including one in which negative values of x were arbitrarily set to 0, the simple quadratic $g(x) = x^2$ and an exponential $g(x) = e^x$. The results of the algorithm using these different transformations were very similar. We only present the results of the algorithm using the exponential transformation.

Given a certain set of synergies, the set of best-fit weighting coefficients, c_{ij}, was found using the non-negative least-squares algorithm[20] supplied by Matlab. This algorithm finds the set of nonnegative coefficients that minimizes the error between the predicted and observed responses, given a particular set of synergies. This procedure is similar to standard regression techniques except that the weighting coefficients are constrained to be positive.

Once the weighting coefficients were found, the error between the predicted and observed responses was used to update the synergies. The error was minimized using gradient descent, in which the synergies are incrementally changed to reduce the prediction error. The change in the synergies was calculated as Eq. 2:

$$\Delta w_i = \sum_j \mu (m_j^{obs} - m_j^{pre})\, c_{ij} g'(w_i) \qquad (2)$$

where g' is the first derivative of the transformation used in Eq. 1 and μ determines the step size of the gradient descent. Because the process of minimizing the error using gradient descent is generally very erratic, the step size of the descent is usually set to be low; we used a value of $\mu = .005$. To further ensure smoothness of the error minimization, we used a 'momentum' coefficient, in which the change in synergy at iteration t is equal to the change in the synergy calculated by Eq. 2 plus a fraction (we used .99) of the change in weight at iteration t – 1. This momentum coefficient serves as a type of running average of the synergy changes. These procedures are standard in gradient descent techniques[11,12]. After updating the synergies, they were normalized so that the vector norm of each synergy was equal to one. The best-fit weighting coefficients were then again found using these new synergies, the synergies updated, and the process repeated.

We applied this algorithm to 90% of the data for each animal, chosen randomly from the responses evoked from the sites in Fig. 1a. After each iteration, we assessed the ability of the synergies found by the algorithm to predict the remaining 10% of responses. When the amount of variance explained by the derived synergies in this set of test data decreased for 20 consecutive iterations, we considered the algorithm to have converged. This procedure reduces overfitting by the algorithm. We repeated the algorithm on 10 different sets of 90% of the data for each animal with different initial synergies for each repetition, to examine effects of different initial conditions on the results of the algorithm. Qualitative analyses suggested that the algorithm required around 50–100 responses to produce consistent results. The algorithm was applied to the entire data sets from each animal, ranging between 177 and 688 responses.

We calculated the similarity between two synergies found by the algorithm as the normalized dot product between them. This value ranges between zero and one, with one representing identical synergies. To establish correspondences between two different sets of synergies, we took all possible dot products between the two sets of synergies. A synergy from one set was matched to the synergy in the other set with which it had its largest dot product. The process of correspondence was also inspected visually in case of ambiguities.

We also applied the k-means algorithm to the set of evoked responses[11,12]. This algorithm is similar to the algorithm described above except that the c_{ij} are equal to zero for all except one synergy.

The algorithm described above is generally similar to factor analytic models[21], with the difference that both the factor loading and factor scores are constrained to be positive. It is also similar to that described[22] except that we are not explicitly imposing a particular prior distribution for the weighting coefficients. We therefore implicitly impose a uniform distribution.

We describe the results of the algorithm using four synergies to fit the data for the following reasons. First, we did a principal components analysis on this data and found that the smallest number of components necessary to explain at least 90% of the variance in each animal was four. Similarly, four synergies were needed for the algorithm used here to explain at least 90% of the variance. Adding an additional synergy to the algorithm explained only an extra 3% of the variance. Finally, applying the algorithm with four synergies corresponded well to a visual inspection of the data and gave consistent results between different animals.

Acknowledgements

We thank Sandro Mussa-Ivaldi and Andrea d'Avella for reading versions of this manuscript and Simon Giszter, Peter Dayan, Kuno Wyler and James Galagan for suggestions. M.C.T. was supported by a HHMI predoctoral fellowship. This research was supported by NIH NS09343 and ONR N00014-95-I0445 to E.B.

Received 30 September; accepted 30 November 1998

1. Bernstein, N. *The Coordination and Regulation of Movements* (Pergamon Press, New York, 1967).
2. Lee, W. A. Neuromotor synergies as a basis for coordinated intentional action. *J. Motor Behav.* **16**, 135–170 (1984).
3. Macpherson, J. M. in *Motor Control: Concepts and Issues* (eds. Humphrey, D. R. & Freund, H.-J) 33–47 (Wiley, Chichester, 1991).
4. Sherrington, C. S. Flexion-reflex of the limb, crossed extension-reflex and reflex stepping and standing. *J. Physiol.* (*Lond.*) **40**, 28–121 (1910).
5. Grillner, S. in *Handbook of Physiology*, sec. 1, vol. 2 (ed. Brooks, V. B.) 1179–1236 (American Physiological Society, Bethesda, MD, 1981).
6. Stein, P. S. G. & Smith J. L. in *Neurons, Networks, and Motor Behavior* (eds. Stein P. S. G., Grillner, S., Selverston A. I. & Stuart D. G.) 61–73 (MIT Press, Cambridge, MA, 1997).
7. Jacobs, R. & Macpherson, J. M. Two functional muscle groupings during postural equilibrium tasks in standing cats. *J. Neurophysiol.* **76**, 2402–2411 (1996).
8. Bizzi, E., Mussa-Ivaldi, F A. & Giszter S. F. Computations underlying the production of movement: a biological perspective. *Science* **253**, 287–291 (1991).
9. Giszter, S. F., Mussa-Ivaldi, F. A. & Bizzi, E. Convergent force fields organized in the frog spinal cord. *J. Neurosci.* **13**, 467–491 (1993).
10. Mussa-Ivaldi, F. A., Giszter, S. F., & Bizzi, E. Linear combinations of primitives in vertebrate motor control. *Proc. Natl. Acad. Sci. USA* **91**, 7534–7538 (1994).
11. Bishop, C. M. *Neural Networks for Pattern Recognition* (Oxford Univ. Press, Oxford, 1995).
12. Hertz, J., Krogh, A. & Palmer R. G. *Introduction to the Theory of Neural Computation* (Addison-Wesley, Reading, MA 1991).
13. d'Avella, A. & Bizzi, E. Low dimensionality of supraspinally induced force fields. *Proc. Natl. Acad. Sci. USA* **95**, 7711–7714 (1998).
14. Fleshman, J. W., Lev-Tov, A. & Burke, R. E. Peripheral and central control of flexor digitorum longus and flexor hallucis longus motoneurons: the synaptic basis of functional diversity. *Exp. Brain Res.* **54**, 133–149 (1984).
15. Pratt, C. A., Chanaud, C. M. & Loeb, G. E. Functionally complex muscles of the cat hindlimb. IV. Intramuscular distribution of movement command signals and cutaneous reflexes in broad, bifunctional thigh muscles. *Exp. Brain Res.* **85**, 281–299 (1991).
16. Schouenborg, J. & Kalliomaki, J. Functional organization of the nociceptive withdrawal reflexes I. Activation of hindlimb muscles in the rat. *Exp. Brain Res.* **83**, 67–78 (1990).
17. Schouenborg, J. & Weng, H.-R. Sensorimotor transformations in a spinal motor system. *Exp. Brain Res.* **100**, 170–174 (1994).
18. Schouenborg, J., Weng, H.-R. & Holmberg, H. Modular organization of spinal nociceptive reflexes: a new hypothesis. *News Physiol. Sci.* **9**, 261–265 (1994).
19. Berkinblitt, M. B., Feldman, A. G. & Fukson, O. I. Adaptability of innate motor patterns and motor control mechanisms. *Behav. Brain Sci.* **9**, 585–638 (1986).
20. Lawson, C. L. & Hanson, R. J. *Solving Least Squares Problems*. (Prentice-Hall, Englewood Cliffs, NJ, 1974).
21. Harman, H. H. *Modern Factor Analysis* (Univ. of Chicago Press, Chicago, 1976).
22. Olshausen, B. A. & Field, D. J. Emergence of simple-cell receptive field properties by learning a sparse code for natural images. *Nature* **381**, 607–609 (1996).